

Heterodyne Interferometer for In-plane and Out-of-plane Displacement Measurements

Hung-Lin Hsieh, Wei-Cheng Wang, Ssu-Wen Pan

Department of Mechanical Engineering, National Taiwan University of Science and Technology, No.43, Sec. 4, Keelung Rd., Da'an Dist., Taipei 106, Taiwan

Keywords: Displacement Measurement, Grating, Heterodyne, In-plane, Out-of-plane.

Abstract: An innovative interferometer based on the heterodyne interferometry, grating shearing interferometry, and Michelson interferometry for precise displacement measurement is proposed. The system configuration is simple and easy to set-up. A heterodyne light beam is generated by using an Electro-Optic Modulating (EOM) technique for amplitude modulation. While the heterodyne light beam normally passes through a semi-transmission diffraction grating, the reflection part (Michelson interferometry) for out-of-plane displacement detection and the diffraction part (Grating interferometry) for in-plane displacement detection can then be obtained. The experimental results demonstrate the system has the capability of providing two-dimensional displacement information simultaneously. The measurement resolution and range can achieve to nanometer and millimeter levels.

1 INTRODUCTION

Nanotechnologies play an important role in modern technology. It includes several research fields, such as medical science, electronics, optics, mechanics, material science and chemistry (Zajtchuk, 1999); (Yu Meyyappan, 2006); (Léron del et al., 2009); (Zhao et al., 2010); (Thillya et al., 2009); (Li et al., 2006). With the further development of these applications, there is an increasing demand for precision displacement measurement methods providing both high measurement resolution and long measurement range. Many measurement techniques have been proposed and developed for precise displacement measurement.

In general, displacement measurement techniques can be divided into two categories, the contact and the non-contact types (Hsieh, 2011). One of the most commonly used contact type techniques is strain gauge. The measurement resolution of strain gauge can achieve nanometric level (Witt, 1974). However, the measurement range of the strain gauge is only capable of achieving micrometric range, which is not suitable for long-range applications. Another commonly used technique of contact type measurement techniques is linear encoder. It is a sensor paired with a scale that used to encode position. The measurement

resolution and range of linear encoder can achieve to nanometric and millimetric levels (Miyajima et al., 1998). But there exists a measurement error caused by misalignment of the two scales of linear encoder which is hard to be eliminated. Moreover, most contact type measurement techniques are unsuitable to apply on the small-scale sample or stage and sometimes will destroy the surface of the sample. These are exactly the disadvantages that limit the application of the contact type measurement techniques.

Laser interferometry is one of the non-contact type measurement techniques, which has been extensively developed to overcome the problems above. The technique has the advantages of high resolution, wide measurement range, and flexible of optical arrangement. Many types of interferometers are designed and used to achieve nanometric-levels precision for long measurement range. But if high frequency noise is considered, sub-nanometer resolution can only be achieved by using heterodyne interferometry. However, the interferometry used without isolation system always suffers from large disturbance or noise, most commonly from background vibration, atmospheric influences, and thermal drift. Measurement accuracy is influenced due to these phenomenons.

Grating interferometers (GIs) are not subject to

these disturbances mentioned above because of the measurement principles are independent of the wavelength of light source. Therefore, GI has better immunity against to the environmental disturbances as compare with heterodyne interferometers. Various GIs for precise measurement have been proposed. Among them, most are for one-dimensional (1D, in-plane or out-of-plane) displacement measurement. For two-axis positioning applications, two-dimensional (2D, in-plane and out-of-plane) displacement measurements are essential. The demand of 2D displacement applications are strong growing, rising attentions for researchers to find methods for in-plane and out-of-plane displacement measurements. Thus the requirements of the measurement techniques should no longer be limited for just 1D use only but also for 2D measurement. Normally, a pair of interferometers, which are perpendicular to each other, can be used for in-plane and out-of-plane displacement measurements respectively. However, the orthogonality of the two interferometers is essential to provide precisely, otherwise the measurement error caused by orthogonal alignment of two interferometers will be induced.

In this paper, a heterodyne interferometer is proposed to measure the motion behavior of a semi-transmission grating in 2D plane, in-plane and out-of-plane. The in-plane displacement information is obtained by grating interferometry and determined by the relation of the grating pitch and optical phase variation. Moreover, the out-of-plane displacement information is acquired by Michelson interferometry which is determined by the relation of the wavelength of light source and the optical path difference. Benefiting from the proposed heterodyne interferometer, this method has the advantages of simple configuration, high measurement resolution, large measurement range, and relatively straightforward operation. The feasibility is demonstrated.

2 PRINCIPLES

The following section will describe the principles of our proposed interferometer. The schematic diagram of the optical arrangement is shown in figure 1. The Y axis indicates the direction of beam propagation and the X and Z axes follow the horizontal and vertical planes. By using Su's electro-optic modulating technique (Su et al., 1996), the complex amplitude (E_0) of the heterodyne light source can be written as follows

$$E_0 = \begin{pmatrix} \exp(\frac{i\omega t}{2}) \\ \exp(\frac{-i\omega t}{2}) \end{pmatrix} \quad (1)$$

where ω is the heterodyne frequency.

2.1 Principle of Grating Interferometry for In-Plane Displacement Measurement

As the heterodyne light beam enters a semi-transmission grating, the beam will be diffracted and propagate in according angle. The angle of diffracted beam can be obtained by the following equation:

$$\alpha_m = \sin^{-1}(\frac{m\lambda}{\Lambda} - \sin \alpha_m) \quad (2)$$

where m is the diffraction order, λ represents the wavelength of the incident beam, Λ and α_m are the grating pitch and the angle between the incident beam and the normal to the grating. In our system, the +1 order diffraction beams are utilized. The electric fields of +1 order diffraction beams can be written as:

$$E_{\pm 1} \propto \exp(ikl_{\pm 1} \pm i\theta_i) E_0 = \begin{pmatrix} \exp(ikl_{\pm 1} \pm i\theta_i + \frac{i\omega t}{2}) \\ \exp(ikl_{\pm 1} \pm i\theta_i - \frac{i\omega t}{2}) \end{pmatrix} \quad (3)$$

The +1 order diffraction beams are incident into two mirrors and then reflected into a polarizing beam-splitter (PBS) respectively. The PBS split the incident two beams into s-polarized status and p-polarized status respectively. As a result, the two beams are divided into four beams. According to the optical arrangement and Jones calculation, the status of the four beams can be written as follows:

$$E_{+1p} = AN(45^\circ)PBS(0^\circ)E_{+1} \propto \exp\left(\frac{i\omega t}{2} + ikl_{+1} + i\varphi_g\right) \times \begin{pmatrix} 1 \\ 1 \end{pmatrix} \quad (4)$$

$$E_{+1s} = AN(45^\circ)PBS(90^\circ)E_{+1} \propto \exp\left(\frac{-i\omega t}{2} + ikl_{+1} + i\varphi_g\right) \times \begin{pmatrix} 1 \\ 1 \end{pmatrix} \quad (5)$$

$$E_{-1p} = AN(45^\circ)PBS(0^\circ)E_{-1} \propto \exp\left(\frac{i\omega t}{2} + ikl_{-1} - i\varphi_g\right) \times \begin{pmatrix} 1 \\ 1 \end{pmatrix} \quad (6)$$

$$E_{-1s} = AN(45^\circ)PBS(90^\circ)E_{-1} \propto \exp\left(\frac{-i\omega t}{2} + ikl_{-1} - i\varphi_g\right) \times \begin{pmatrix} 1 \\ 1 \end{pmatrix} \quad (7)$$

Refer to Eq. (4)-(7), E_{+1p} , E_{+1s} , E_{-1p} and E_{-1s} represent the electric fields of the four beams, φ_g is phase difference induce by the moving grating. After passing a polarizer with 45° polarized, the +1 order

diffraction beams interfere. The interference beatings are then detected by two detectors (PD3 and PD4) and can be shown below

$$I_3 = |E_{+1p} + E_{-1s}|^2 = \frac{1 + \cos[\omega t + k(l_{+1} - l_{-1}) + 2\varphi_g]}{2} \quad (8)$$

$$I_4 = |E_{+1s} + E_{-1p}|^2 = \frac{1 + \cos[\omega t + k(l_{-1} - l_{+1}) - 2\varphi_g]}{2} \quad (9)$$

Then the detected signals (I_3 and I_4) are sent into a lock-in amplifier (LIA) so the phase difference between the two signals can be obtained as:

$$\varphi_g = \frac{4\pi\Delta l}{\Lambda} \quad (10)$$

where Δl is the grating displacement, Λ represents the grating pitch. As a result, the grating displacement can be written as:

$$\Delta l = \left(\frac{\varphi_g}{4\pi}\right) \times \Lambda \quad (11)$$

2.2 Principle of Michelson Interferometry for out-of-Plane Displacement Measurement

In our system, a beam-splitter was added in front of the grating. The semi-transmission grating was regarded as a reflective mirror in this detection configuration so the out-of-plane displacement can be detected by using a Michelson interferometry. The optical arrangement is shown in figure 1. A He-Ne laser beam is incident into a beam-splitter (BS). The beam is split into two parts, which are reference and measurement beams. The reference beam is incident into a fixed mirror then reflected directly into the detector (PD1). The measurement beam is incident into a grating and reflected by the semi-transmission grating. As a result, the grating can be regarded as a mirror, and the beam reflected by grating is called measurement beam. Since the beam is reflected by grating, the configuration of Michelson interferometry has been easily constructed.

The electric fields of the reference and measurement beams are shown below

$$E_r = EOM(\omega t)E_m = \begin{pmatrix} \exp\left(\frac{i\omega t}{2} - ikl_r + i\theta_r\right) \\ \exp\left(\frac{-i\omega t}{2} - ikl_r + i\theta_r\right) \end{pmatrix} \quad (12)$$

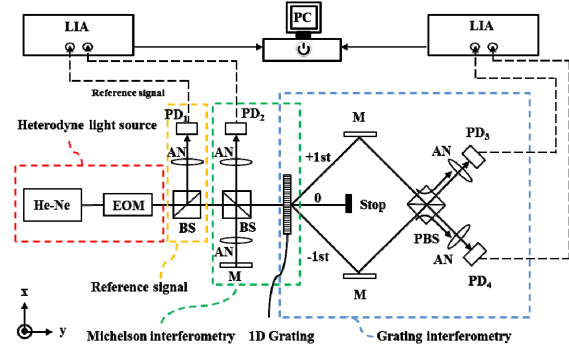


Figure 1: The optical configuration of proposed system. (EOM: Electro-optic modulator; AN: Analyzer; PD: Photodetector; M: Mirror; BS: Beam splitter; PBS: Polarizing beam splitter; LIA: Lock-in Amplifier.)

$$E_m = EOM(\omega t)E_{in} = \begin{pmatrix} \exp\left(\frac{i\omega t}{2} - ikl_m + i\theta_i\right) \\ \exp\left(\frac{-i\omega t}{2} - ikl_m + i\theta_i\right) \end{pmatrix} \quad (13)$$

where l_r and l_m are the optical paths of the reference and measurement beams respectively. After passing a polarizer with 45° polarized, the two beams interfere and can be measured by the detector (PD2). The interference signal is shown as

$$I = |E_r + E_m|^2 \propto \cos[k(l_2 - l_1)] \quad (14)$$

After sending the interference signals into the LIA, the phase difference signal can be obtained as

$$\Delta\theta = k(l_2 - l_1) = k \times 2\Delta l \quad (15)$$

$$\Delta l = \frac{\Delta\theta}{2k} \quad (16)$$

Refer to Eq. (16), the out-of-plane displacement Δl can be obtained.

3 EXPERIMENTAL RESULTS

To demonstrate the feasibility of our proposed interferometer, two measurement experiments were performed for in-plane and out-of-plane displacement measurements and for further application the straightness also been tested. It relies on a heterodyne beam source composed of a linearly polarized He-Ne laser beam modulated by an electro-optic modulator (EOM) (model: EO-PM-NR-C1). The frequency difference between the s- and p- polarizations of the heterodyne light source is 20 kHz. A commercial semi-transmission grating with a pitch size of $1.2 \mu\text{m}$ was mounted on a two

axes positioning stage. A BS is placed in front of the grating so the beam can be split into two detection parts, reflection and diffraction detection types. The two detection types were used to measure out-of-plane and in-plane displacements respectively. Two LIAs (SR850) with an angular resolution of 0.001° were used to measure the phase difference between the reference signal and each of the interference signals.

3.1 Displacement Measurement Result

A displacement test was performed to demonstrate that our proposed interferometer is capable of sensing in-plane and out-of-plane displacements. The positioning stage was asked to move forward and backward with amplitude of $100\ \mu\text{m}$ along in-plane and out-of-plane directions respective. Figure 2 shows the experimental result of X (in-plane) direction obtained by the grating interferometry. The curve obtained by grating interferometry is similar to the driving signal. Also, the experimental result of Y (out-of-plane) direction obtained by Michelson interferometry is shown in figure 3. As shown in figure 3, the curve obtained by Michelson interferometry is as linear as the driving signal we used. From the two experimental results, it is clearly that our proposed system has the ability to measure in-plane and out-of-plane displacements.

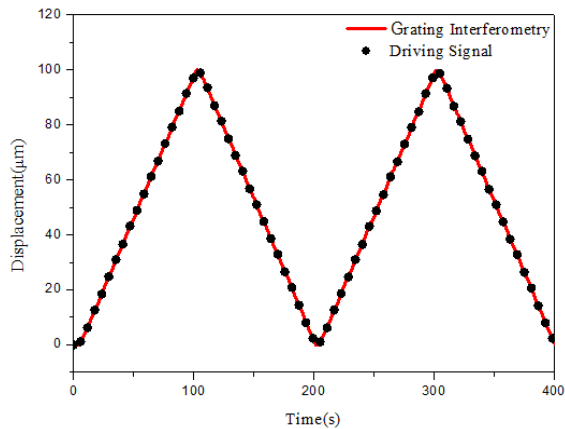


Figure 2: Displacement measurement result of X direction ($100\ \mu\text{m}$).

3.2 Straightness Measurement Result

Furthermore, a straightness measurement experiment was performed to demonstrate that our interferometer can be used to measure straightness error in two directions. In this experiment, the positioning stage was set to move along the X

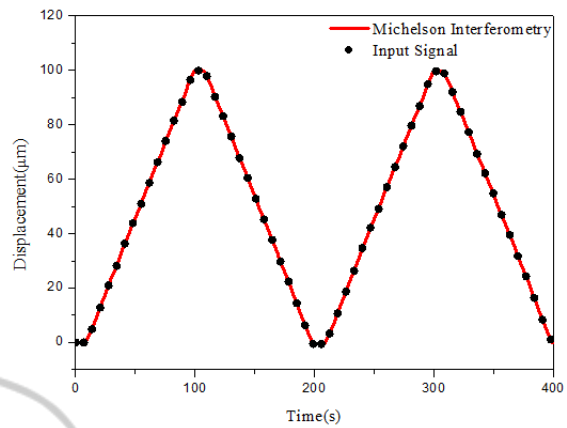


Figure 3: Displacement measurement result of Y direction ($100\ \mu\text{m}$).

direction, the lateral displacement (straightness error) in the Y direction was recorded by Michelson interferometry. The experimental result is shown in figure 4. Clearly, the maximum straightness error is about $700\ \text{nm}$ in the Y direction within the stroke of $4\ \text{mm}$ along the X direction. The experimental data also show a pair of similar back (solid black squares) and forth (solid red circles) paths. Besides measuring straightness error along the X direction, the experiment of straightness error along the Y direction was also performed. Figure 5 shows the measurement result of straightness error obtained by grating interferometry. The measurement result shows that a pair of similar back-and-forth paths. The maximum straightness error is about $300\ \text{nm}$ in the X direction within the stroke of $4\ \text{mm}$ along the Y direction. According to the above experimental results, it demonstrates that our proposed interferometer is capable of measuring straightness in both directions (X and Y) successfully.

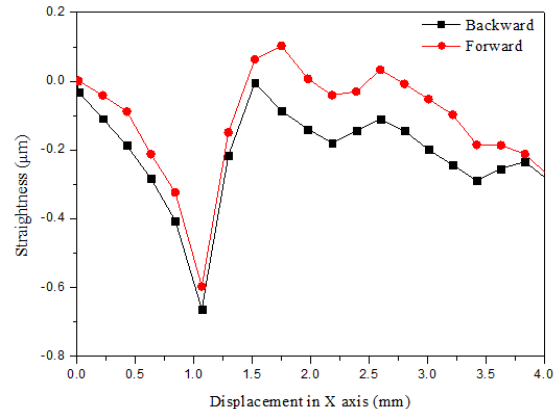


Figure 4: Straightness measurement result of X direction.

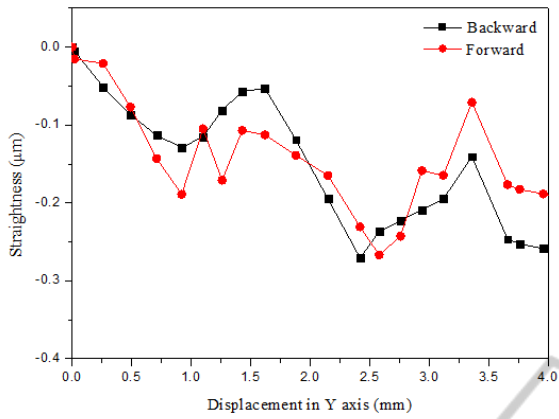


Figure 5: Straightness measurement result of Y direction.

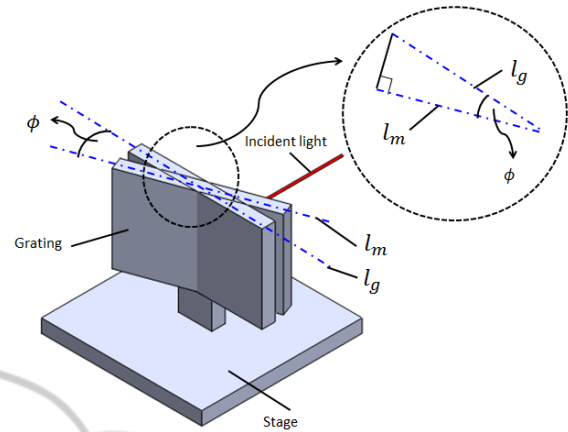


Figure 6: error induced by tilted grating.

4 DISCUSSION

In our proposed system, the measurement error caused by the misalignment angle of yaw error will influence the measurement result. In additions, because our method combines heterodyne interferometry and grating interferometry, we need to take into account the error effects coming from both of those interferometries. In our case, the error arises from non-linearity of heterodyne modulating technique and non-uniformity of grating pitch. These errors also will affect our measurement result. As a result, in this section, we are going to discuss the effect of these factors above.

4.1 Error Caused by the Misalignment Angle of Yaw Error in the Grating Interferometry

As shown in figure 6, if there exists a misalignment angle of yaw error between the grating and the positioning stage, the displacement measured by the grating interferometry will be influenced. The relationship between the measured displacement l_m and the actual displacement l_g is shown below.

$$l_m = l_g \cos \phi \quad (17)$$

The error caused by the misalignment can be written as

$$e_g = l_g - l_m = l_g - l_g \cos \phi = l_g (1 - \cos \phi) \quad (18)$$

If the yaw error factor is estimated to be 0.05° while the stage is asked to move a displacement of 1 mm, the measurement error is about 0.38 nm in this case.

4.2 Error Caused by the Misalignment Angle of Yaw Error in the Michelson Interferometry

As shown in figure 7(a), if there exists a misalignment angle of yaw error between the grating and the positioning stage, the displacement measured by the Michelson interferometry will also be influenced. The $l_a + l_c$ and $l_b + l_d$ represent the optical paths of the measurement beams with and without yaw errors respectively. The relationship between l_a and l_b can be written as

$$l_b = l_a \frac{\sin 135^\circ}{\sin(45^\circ - 2\phi)} \quad (19)$$

And the relationship between l_d and l_c can be written as

$$l_d = l_c \frac{\sin 45^\circ}{\sin(135^\circ - 2\phi)} \quad (20)$$

Therefore, the measurement error (e_p) caused by the misalignment can be written as follow

$$e_p = (l_b + l_d) - (l_a + l_c) \quad (21)$$

If there exists a misalignment angle of yaw error of 0.05° , the measurement error is about 1.747 nm in this case.

4.3 Error Caused by non-linearity of Heterodyne Modulating Technique and Non-Uniformity of Grating Pitch

The non-linearity in a typical heterodyne interferometry mainly arise from the mixing of

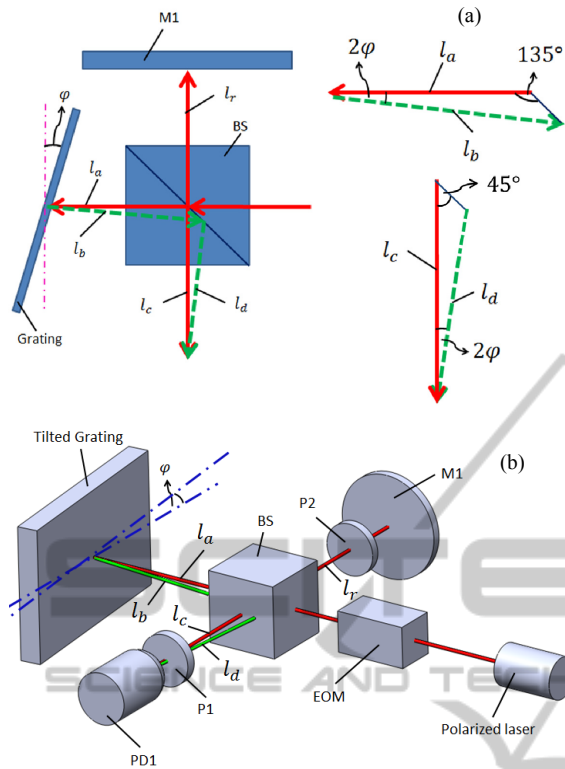


Figure 7: The Error Effect of Michelson Interferometry: (a) the top view of the error configuration, (b) the overall error configuration

frequency and polarization. Moreover, non-uniformity is caused by utilizing a grating with irregular grating pitch or the thermal variation in grating interferometry. The performance of our proposed system is influenced by these factors. The theoretical displacement error $|\Delta e_t|$ in the proposed interferometer is given by the following expression:

$$|\Delta e_t| = \frac{\Phi_g}{4\pi} |\Delta\Lambda| + \frac{\Lambda}{4\pi} |\Delta\Phi_g| \quad (22)$$

where $|\Delta\Lambda|$ is the uncertainty of grating pitch and $|\Delta\Phi_g|$ is the phase uncertainty mainly caused by frequency mixing and polarization mixing errors. According to the characteristic of the experimental setup, the total error $|\Delta e_t|$ caused by non-linearity and non-uniformity is about 1.628 nm.

5 CONCLUSIONS

In this research, we proposed a heterodyne interferometer for measuring 2D (in-plane and out-of-plane) displacement. Once a heterodyne light beam normally passes through a semi-transmission diffraction grating, the system is divided into two

detection parts, reflection part (Michelson interferometry) and diffraction part (Grating interferometry). The experimental results show that the system has ability to provide precise in-plane and out-of-plane displacement information without changing its optical arrangement. Straightness tests in 2D are also conducted to prove the system feasibility. Moreover, the error analysis reveals that the dominant errors are mainly caused by the misalignment of the yaw angle, the errors arising from non-linearity of heterodyne modulating technique and the non-uniformity of grating pitch. Therefore, the measurement resolution and range can achieve to nanometric and millimetric levels.

ACKNOWLEDGEMENTS

The authors cordially thank the NTUST Opto-Mechatronics Technology Center for their useful help. This study was supported by the National Science Council, Taiwan, under contract NSC-101-2218-E-011-033.

REFERENCES

- Zajtchuk R., 1999. "New technologies in medicine: biotechnology and nanotechnology" Disease a-Month, Volume 45, Issue 11, PP453-495.
- B, Yu, M. Meyyappan, 2006 "Nanotechnology: Role in emerging nanoelectronics" Solid-State Electronics, Volume 50, Issue 4, PP536-544.
- G. Léron del, A. Sinno, L. Chassagne, S. Blaize, P. Ruaux, A. Bruyant, S. Topçu, P. Royer, Y. Alayli, 2009 "Enlarged near-field optical imaging" Applied Physics, Volume 106, Issue 4, PP 044913 - 044913-4.
- J. Zhao, M. Kunieda, G. Yang, X. Yuan, 2010 "The Application of Nanotechnology for Mechanical Manufacturing," Key Engineering Materials, Volumes 447 - 448, PP86-90.
- L. Thillya, S. Petegemb, P. Renaulta, F. Lecouturiere, V. Vidald, B. Schmittb, H. Swygenhovenb, 2009 "A new criterion for elasto-plastic transition in nanomaterials: Application to size and composite effects on Cu-Nbnanocompositewires," Acta Materialia, Volume 57, Issue 11, PP3157-3169.
- J. Li, Y. Lu, M. M, 2006 "Nano Chemical Sensors with Polymer-Coated Carbon Nanotubes," IEEE Sensors Journal, Volume 6, Issue 5, PP 1047-1051.
- H. L. Hsieh, 2011 "Novel interferometric stage based on quasi-common-optical-path configuration for large scale displacement," doctoral thesis.
- G. R. Witt, 1974 "Thin solid film," Thin Solid Films Volume 22, Issue 2, pp133-156.
- H. Miyajima, E. Yamamoto, K. Yanagisawa,

1998” *Optical micro encoder with sub-micron resolution using a VCSEL*” *Sensors and Actuators A: Physical*, Volume 71, Issue 3 pp213–218.
D. C. Su, M. H. Chiu, and C. D. Chen, 1996 "*Simple two-frequency laser*," *Precis. Eng.* 18, 161–163.

